Politecnico di Torino

BIOENGINEERING OF REHABILITATION

Master's Degree in Biomedical Engineering

A.Y. 2022 - 2023

REPORT

ANALYSIS OF JOINT ANGLES AND MUSCLE ACTIVATIONS DURING WALKING

Mazzoletti Laura (292229)

Richetto Francesco (292281)

Sabbadini Benedetta (292182)

Scimeca Sabrina (279968)

Scorrano Luca (296047)

1. INTRODUCTION and DATASET

The aim of this work is to study joint angles and the corresponding muscle activations during walking. Starting from kinematic and electromyographic data, the relationship between kinematics and muscle activations is assessed.

1.1 Kinematic data

The data provided were studied through the implementation of the Plug In - Gait method drawn up by Vicon: this is a biomechanical model for the lower limbs developed by Kadaba, David and Helen Hayes Hospital.

The model used made it possible to define the reference systems of the lower limbs, based on the subject's anthropometric measurements and the processing of data acquired during walking, by positioning 10 mm diameter markers. A total of 16 markers were placed, 8 per side (indicated by R for the right side and L for the left side), shown below:

- Anterior Superior Iliac spines (RASI - LASI);
- Posterior Superior Iliac Spines (RPSI - LPSI);
- Thight (RTHI - LTHI);
- Knee (RKNE - LKNE);
- Tibia (RTIB - LTIB);
- Ankle (RANK - LANK);
- Heel (RHEE - LHEE);
- Toe (RTOE - LTOE);

The anthropometric measurements provided are the distance between the antero-upper iliac crests (LASI - RASI), average leg length, knee and ankle width.

The frames were acquired at a frequency of 100 Hz, with a total duration of two minutes.

1.2 Electromyographic data

At the same time, EMG signals were acquired by means of bipolar electrodes placed on the leg muscles during the subject's gait. Specifically, EMG traces were analysed for Biceps femoris (BF), Gluteus medius (GMed), Tibialis anterior (TA), Vasto lateralis (VL), Soleus medialis (SOLm) and Gastrocnemius medialis (GM).

For each muscle there is only one trace, with the exception of the medial gastrocnemius, of which fifteen traces were acquired from an electrode array. Each trace had a duration of two minutes, while the acquisition frequency of the EMG signal was 2048 Hz.

2. METHODS

2.1 Calculation of reference systems and centres of rotation of pelvis, femur, ankle and foot

Four functions `calc_references_x.m`, one for each skeletal segment, were constructed for the calculation of the local reference systems, implementing the equations of the Plug - In Gait protocol. After receiving as input the 3D coordinates of the markers relative to the skeletal segment under examination, the structures containing the coordinates (x, y, z) of the local reference system with respect to the global reference system of the laboratory and the coordinates of the centre of rotation are returned as output. The reference systems obtained are orthonormal and saved within the `loc_ref` structure. The centres of rotation are saved within the `JOINTS structure`:

Below are the implemented functions:

- **Pelvis** (`calc_references_pelvis.m`)**:** the origin of the reference system is located at the HJC point (midpoint between the right and left centres of rotation of the hip). The y-axis is identified by a versor directed mid-laterally (from the midpoint towards LASI); the z-axis identifies the inferior-upper axis, while the x-axis is defined as the vector product between the versors of the y-axis and the z-axis, i.e. in the antero-posterior direction.

- **Femur** (`calc_references_femur.m`): The right and left rotation centres define the origin of the reference system for the right and left femur, respectively. The z-axis is defined in the inferior - superior direction; the x-axis is defined in the posterior - anterior direction; the y-axis is calculated as the vector product between the versors of the z-axis and the x-axis: for the left side it has a medial - lateral direction, while for the right side it has the opposite direction, i.e. latero - medial.

- **Ankle** (`calc_references_shank.m`): the centres of rotation of the joint define the origins of the two left and right reference systems. The z-axis is defined as the inferior - superior axis; the x-axis is defined in the posterior - anterior direction; the y-axis is obtained as the vector product between the versors of the z- and x-axes: here too, a distinction is made between the two sides, for the left side it has a medial - lateral direction, while for the right side it has a latero - medial direction.

- **Foot** (`calc_references_foot.m`): The foot reference system is calculated assuming a flat foot. The origin is placed at the TOE marker. The z-axis has an antero - posterior direction (TOE → AJC); the y-axis has a latero - medial direction for the right foot and a medio - lateral direction for the left foot; the x-axis, corresponding to the infero - superior axis, is calculated as the vector product between the versor of the y- and z-axes.

The representation of the resulting reference systems is shown in Fig. 1, obtained through the `animation.m` function.

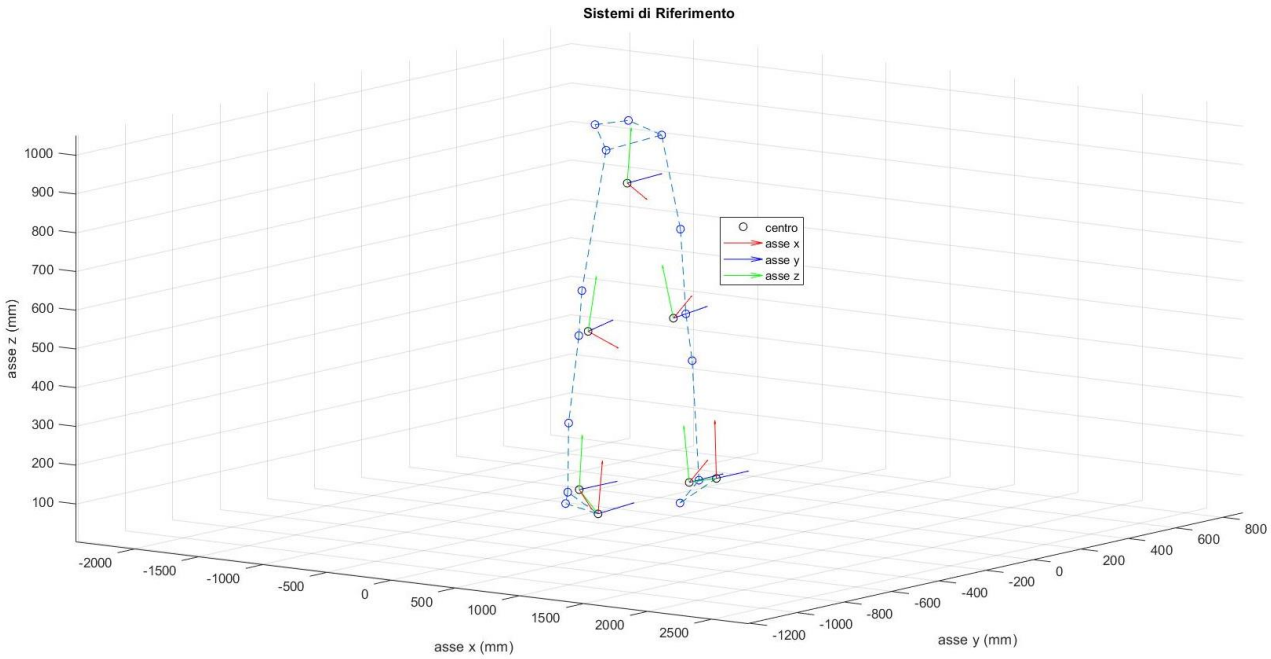

***Figure 1**: Reference systems for the pelvis, right and left knee, right and left foot, resulting from the application of the Plug In Gait model. The markers placed on the subject and used for the acquisition are indicated by the empty dots.*

2.2 Calculation of the rotation matrix and joint angles at the hip, knee, ankle of the left limb

We now proceed to calculate the joint angles between the joints for each instant of acquisition. In order to calculate the joint angle of a joint, the position and orientation of the proximal rigid segment under

examination (hip, knee and ankle) with respect to the nearest distal reference system (i.e. knee, ankle and foot, respectively) is evaluated. In particular, for the calculation of ankle angles, the axes of the foot and ankle reference system were coordinated in the composition of the rotation matrix.

In the study of rigid body dynamics, Euler demonstrated how the relative orientation between two orthogonal co-ordinate systems can be defined from a set of three independent angles, called Eulerian angles. Any orientation of the distal reference system with respect to the proximal reference system can be obtained as the result of three successive and ordered elementary rotations around one of the three axes, regardless of the sequence in which they are applied [1], [2].

Of the various possible combinations, also drawing on what has been reported in the literature [3], the following were performed, in order:

1. A γ rotation about the y-axis;
2. A α rotation about the x-axis;
3. A β rotation about the z-axis.

From the resulting rotation matrix, we obtain the angles

$$\alpha = \sin^{-1}(r_{32}) \qquad \gamma = \sin^{-1}(\frac{-r_{12}}{\cos\alpha}) \qquad \beta = \sin^{-1}(\frac{-r_{31}}{\cos\alpha})$$

Where α is the angle of adduction - abduction, β is the angle of intra - extra rotation and γ is the angle of flexion - extension.

The equations implemented for the calculation of joint angles are given within the function `joint_angles.m`.

2.3 Identification of complete walking cycles

Walk cycles were identified by considering the local minima of the trajectory of the marker positioned on the left heel (LHEE), implementing Matlab's `findpeaks` function.

The step cycle duration was calculated as the difference between samples corresponding to consecutive minima on the z-axis. In order to discriminate complete step cycles, the distance between two consecutive peaks was evaluated, imposing a threshold, calculated as the average of the distances between the peaks: if the step duration is greater than the imposed threshold, we are faced with a turnaround of the subject, which will not be considered since in that time window the subject is partially or totally outside the field of acquisition of the cameras. Therefore, we proceed with counting the number of steps for the current cycle, excluding the step following the turn from the count.

From the calculation of joint angles described above, the angle values obtained are saved within the `ANGLES` structure, which contains three matrices, one for each skeletal segment.

From these, each step is resampled so that each epoch has the same number of samples: in particular, all corner sequences are sampled at 100 samples.

Only useful step cycles are now selected: the first step of each cycle (first step after the turn) is eliminated a priori; steps that are considered incomplete are then removed: if there is at least one `NaN` at an angle value, that step is excluded for all three joints, so that the same number of steps is available for each. The `TREND_ANGLES` structure is created, which saves the complete joint angle variations within it, considering only the selected steps.

The trajectory of the marker placed on the heel and the start and end instant of the step cycle are shown in Figure 2.

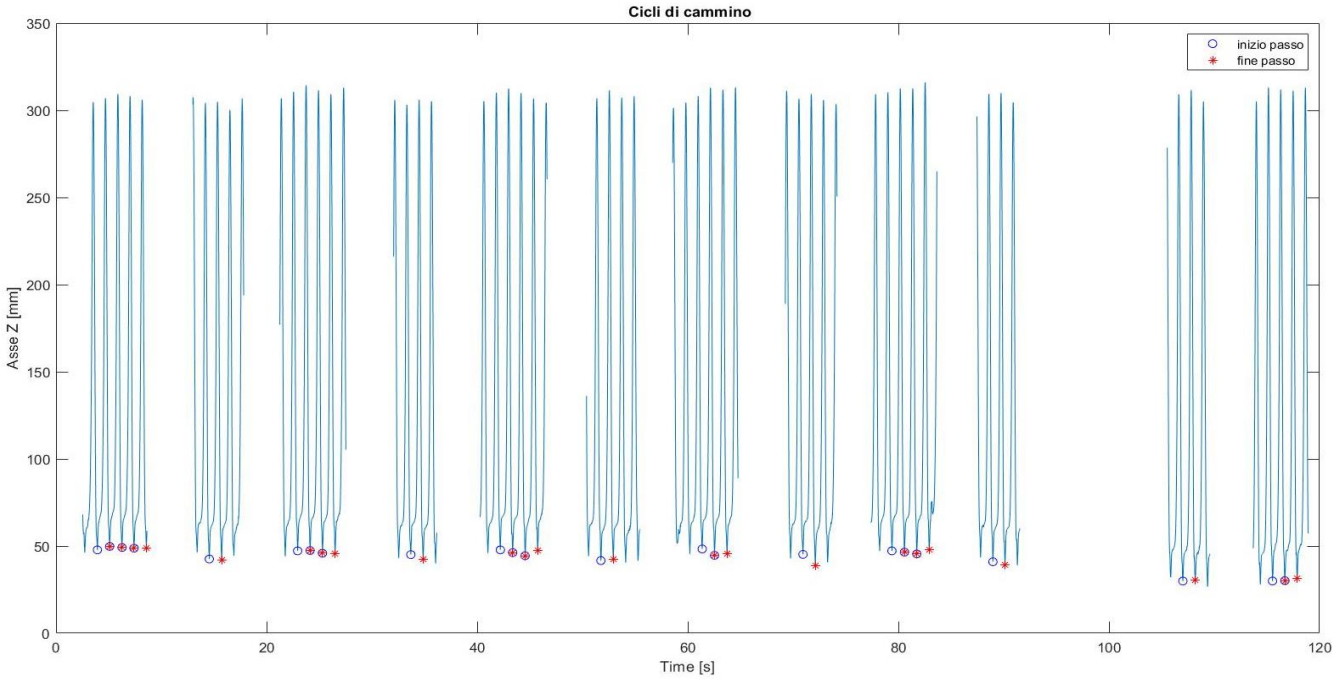

***Figure 2**: Representation of the heel trajectory (LHEE marker), start and end times of the cycle considered.*

2.4 Calculation of the average trend and variability of joint angles

Fig. 3 shows the average joint angle trends evaluated for the left limb. In detail, for each segment, the average variation of the angles as a function of the step cycle percentage and the relative standard error are shown. The flexion-extension, adduction-abduction and intra- extra rotation angles were calculated for each segment.

As found in the literature [3], a dextrorotatory rotation in the sagittal plane (around the z-axis, corresponding to the angle γ), results in hip extension, knee flexion and ankle plantaflexion. A right-turn in the frontal plane (around the x-axis, represented by the angle α) corresponds respectively to an adduction - abduction of hip, knee and an inversion/eversion of ankle. Finally, a rotation in the transverse plane (around the y-axis, defined by the β angle) defines hip, knee and ankle rotation respectively.

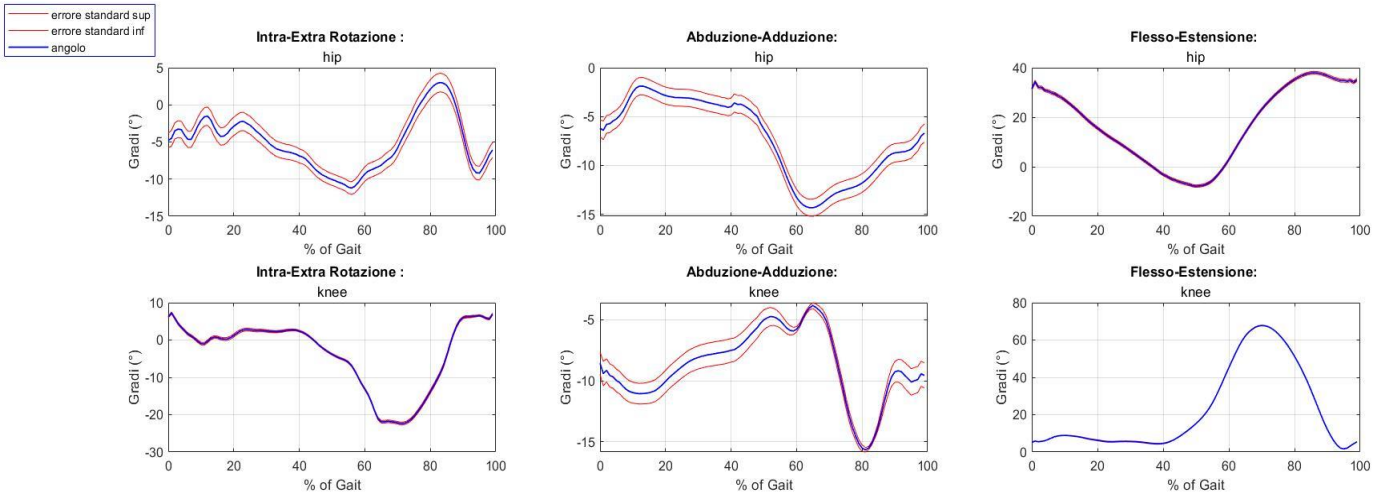

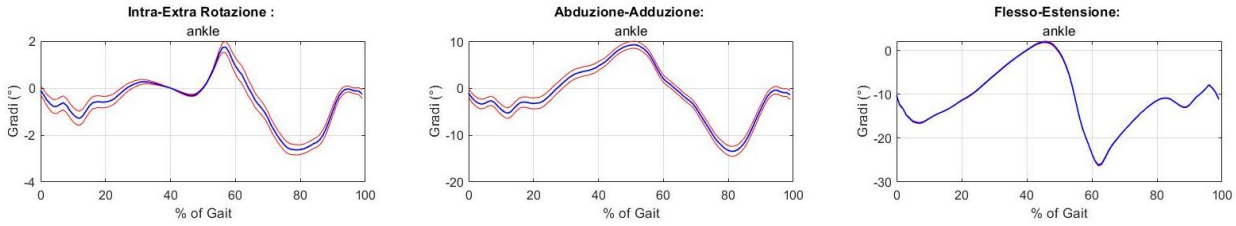

***Figure 3**: Representation of the average trend with relative standard error of the joint angles at the hip, knee and ankle as a function of step cycle percentage.*

2.5 Calculation of the average trend and variability of muscle activations

The analysis of the average trend and variability of the muscle activations was conducted by considering only the step cycles considered to be complete, which were identified previously. The envelopes of the EMG signals were obtained by implementing the `filtering.m` function and saved within the `FILT` structure.

Signal pre-processing. The display of the raw EMG trace shows the absence of some signal sections, probably due to a loss of information during signal transmission: any missing samples (indicated as `NaN`) were interpolated so that the signal could be reconstructed in its entirety. Signal processing, implemented by means of the `filtering.m` function, is carried out: a band-pass filter is introduced for noise removal, with a bandwidth proper to the EMG signal (approx. 10 - 450 Hz). The lower cut-off frequency is set to a value slightly higher than that of the EMG signal band, in order to remove any movement artefacts due to the gel interposed between the electrodes and the skin. An anticausal filtering (`filtfilt`) is then implemented, so as not to introduce phase distortions.

Envelope extraction. Noise-filtered signals are then high-pass filtered, with a cutoff frequency of 35 Hz, rectified, so as to have only positive signals. In order to extract the envelope, low-pass filtering is introduced, with a cutoff frequency set at 3.8 Hz for the noisiest signals (BF, Gmed and TA), while for the rest the cutoff frequency is set at 9 Hz.

Average trend and variability of muscle activations. The envelopes extracted from the EMG signals were then normalised and resampled, so that each signal had the same number of samples, in order to correlate the muscle activation with the gait cycle. In particular, it was chosen to resample the electromyographic signal to 100 samples. Afterwards, the resampled signals were saved in the `FILT_RES` structure, their mean and standard error were calculated. For the GM, the first two proximal channels (Ch1 and Ch2) and the last two distal channels (Ch14 and Ch15) were considered. The results obtained are shown in Fig. 4.

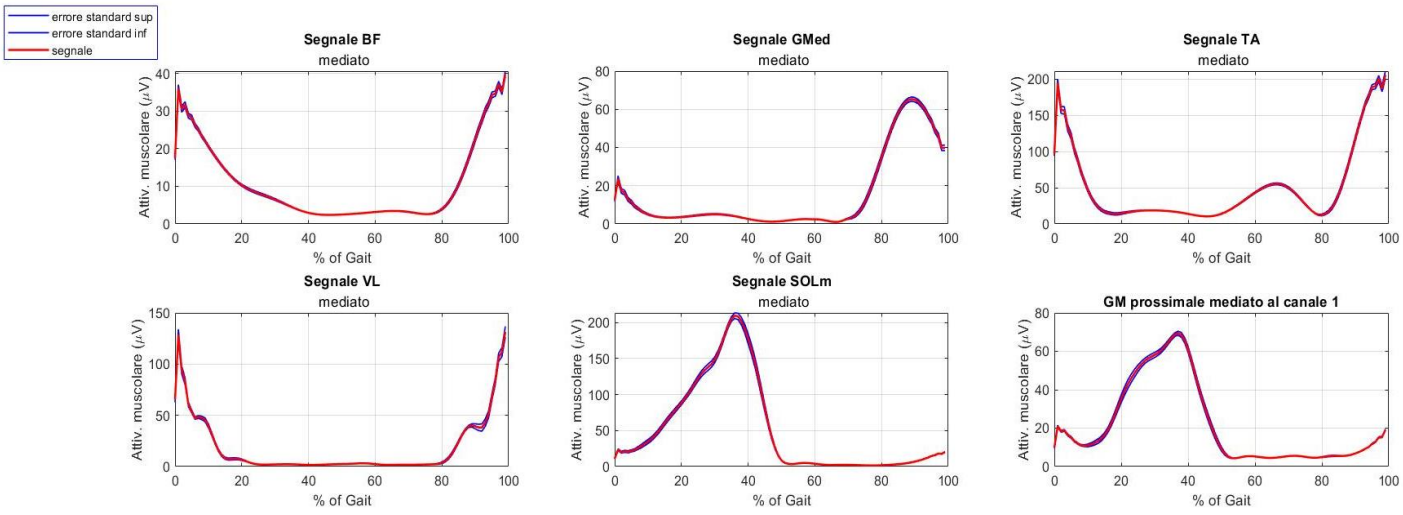

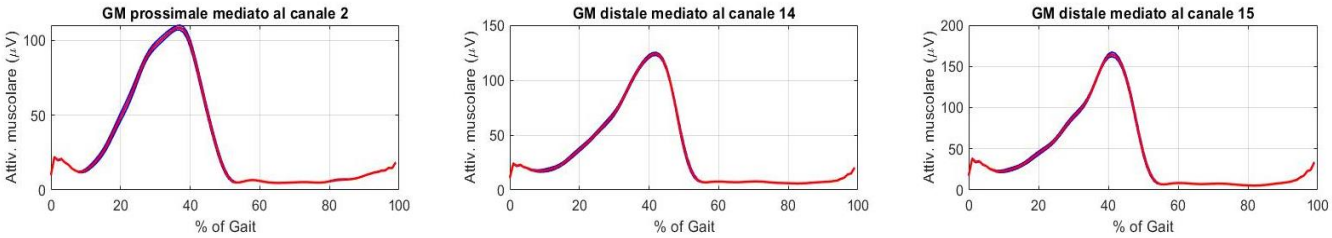

***Figure 4**: Representation of average muscle activations with relative standard error as a function of gait cycle. The muscles taken into analysis are biceps femoris (BF), gluteus medius (Gmed), tibialis anterior (TA), vastus lateralis lateralis (VL), soleus medialis (SOLm), gastrocnemius medialis (GM), of which the first two proximal channels (Ch1 and Ch2) and the last two distal channels (Ch14 and Ch15) were considered.*

3 RESULTS

3.1 Flexion-extension joint angles as a function of gait cycle and their congruence with literature data

The deflection-extension angles derived above are in agreement with the data in the literature, both in terms of the curve's course and angular range [Fig. 5].

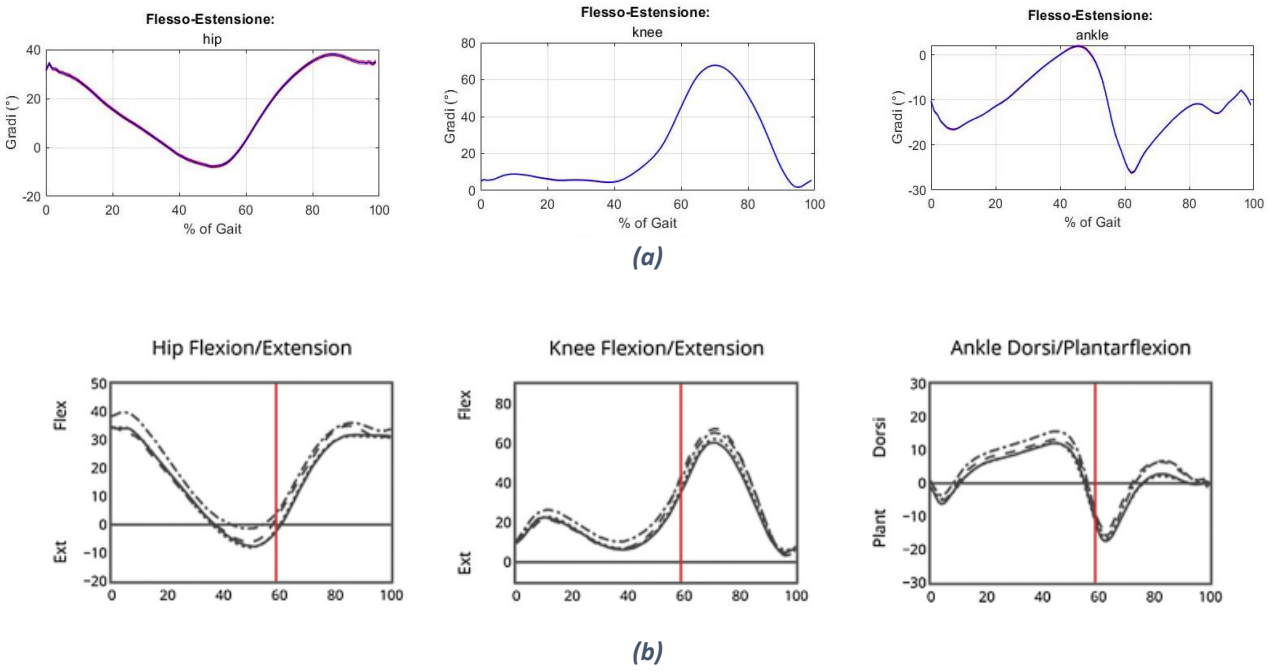

***Figure 5**: Results of the joint angle assessment performed in our analysis (a).*
Visualisation of the flexion-extension joint angles of hip, knee and ankle obtained by examining two different gait models, modified Conventional Gait Model and cluster-based model, with both computational methods 6DoF = six-degrees-of-freedom and IK = inverse kinematics. The vertical line highlights the heel detachment point (b). [4].

During walking, the range of hip flexion-extension angle varies from about 40° at heel strike (maximum flexion), to a maximum extension that exceeds 5° visible in the stance phase, in the instant just prior to heel strike (highlighted by the red vertical line in the figure).

With regard to the angle of the knee joint, in the first part the curve shows a slight flexion, reaching 10 - 20°, which is not very appreciable in our representation, with a slight peak reaching approximately 10°. As a result of stance, the joint extends until the end of hip extension (approx. 40% of the Gait Cycle). A peak indicating maximum flexion (with values around 60° - 70°) in the first phase of the swing can be observed at the stance phase and at the foot take-off.

The change in angle at the ankle comprises a range of approximately 15°, in both dorsiflexion and plantarflexion. Plantarflexion is visible in the first phase of heel strike; with the foot in support, the movement continues with dorsiflexion. The course of the curve reaches its peak at the detachment of the heel. At the detachment of the heel from the ground, there is a rapid plantaflexion and consequent transition to the dorsiflexion configuration: the ankle dorsiflexes in preparation for the stance, preventing the subject from stumbling while advancing the leg. Compared to the literature, the graph obtained, shown in Fig. 5, shows an initial offset, probably due to the fact that a 90° approximation between tibia and foot was assumed.

The following is a schematic representation of the angular changes of the hip, knee and ankle during stepping. [Fig. 6].

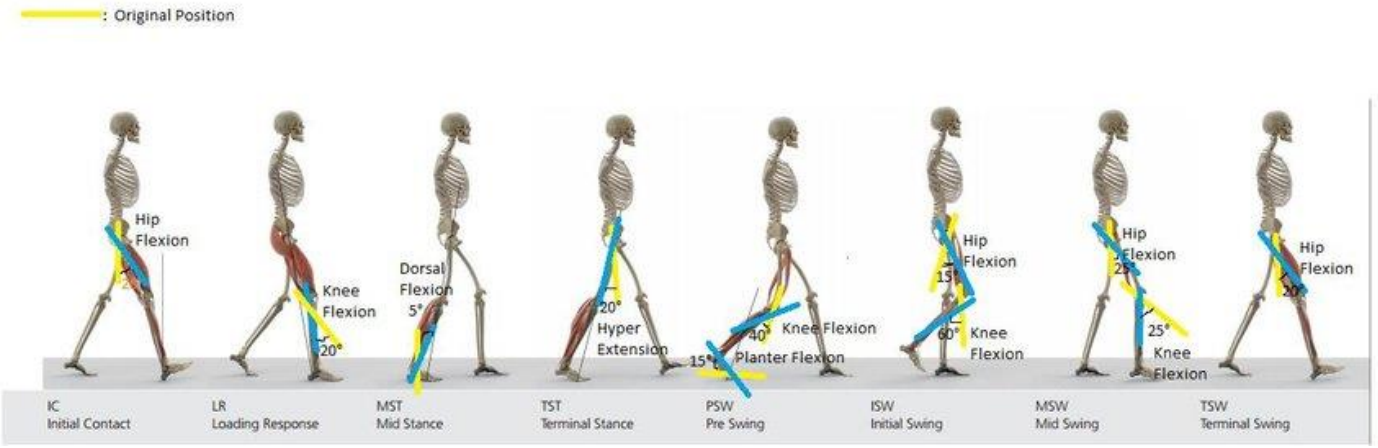

***Figure 6**: Schematic representation of changes in hip, knee and ankle angles during stepping. [5]*

3.2 Muscle activations as a function of the gait cycle and their congruence with literature data

During walking, the muscles most involved are the tibialis anterior, gastrocnemius and soleus: in the initial foot stance phase (0 - 10%, Initial Contact - Foot Flat), the tibialis anterior is active in eccentric contraction to obtain a controlled forefoot stance; in the next phase, the push phase (up to 50 - 60% of the stride cycle, Foot Flat - Heel Off), the tibialis anterior is silent, while the gastrocnemius and soleus, which are mainly responsible for plantar flexion of the foot, are activated. Following the release of the forefoot (Toe Off), the flight phase then begins, in which the anterior tibialis is activated again, which allows the dorsal flexion of the foot to take place, to remain active until the next forefoot stance.

The extracted envelopes of the EMG signals shown in Fig.4 can be considered to be in agreement with the literature: from the comparison, the envelopes of the derived EMG signals show rather similar trends.

In detail, it can be observed that the trends for the soleus medialis (SOLm), vastus lateralis (VL), biceps femoris (BF) and tibialis anterior (TA) are quite similar, while some inconsistencies are evident in the case of gluteus medialis and gastrocnemius. In the case of the medial gluteus, there is a 15-20% discrepancy compared to Fig. 7 and Fig. 8. For the gastrocnemius, there is a discrepancy in the average course between our envelope and that shown in Fig. 8; on the contrary, there is a similarity with the course in Fig. 7. The inequality in the first case may be due to a different positioning of the signal sampling system on the muscle considered.

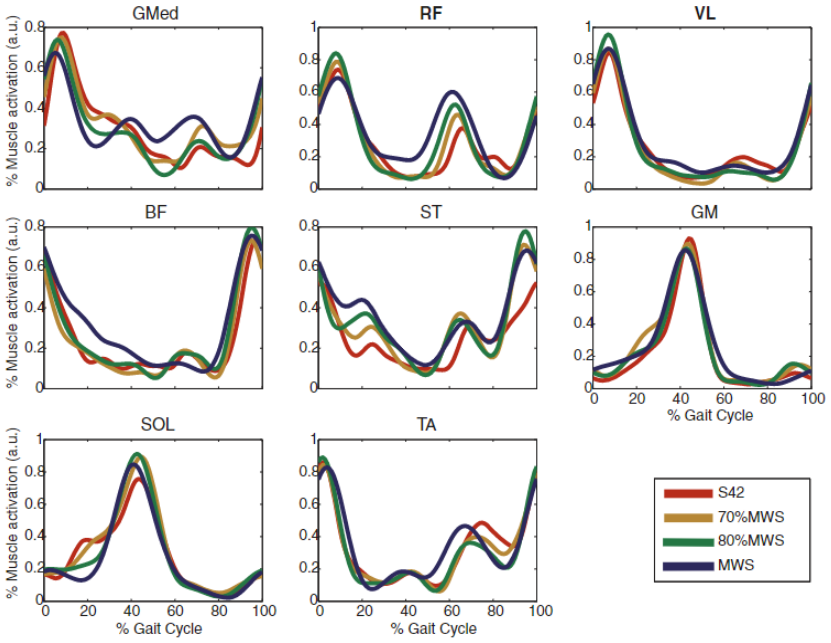

Figure 7: *Muscle activations averaged over 10 gait cycles at different walking speeds expressed as a function of walking percentage (shown on the x-axis). The percentage of muscle activation shown on the y-axis is calculated by dividing each muscle signal by its peak over the 10 gait cycles under examination. For our analysis, the gluteus medius (Gmed), vastus lateralis (VL), biceps femoris (BF), gastrocnemius (GM), soleus (SOL) and tibialis anterior (TA) muscles were considered. [8]*

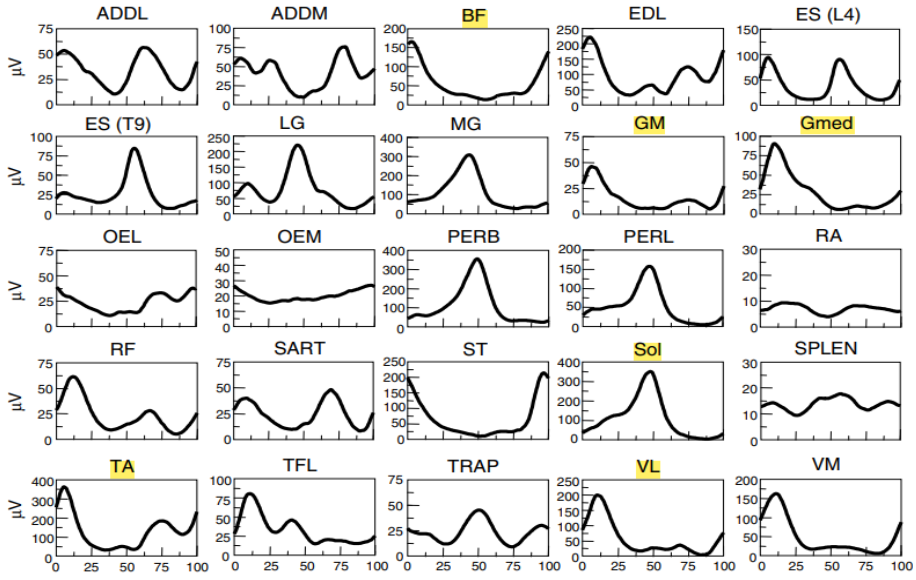

Figure 8: *Muscle-mediated activations on a gait cycle. We highlight the EMG mediated signals of interest for our analysis, relating to biceps femoris (BF), gastrocnemius medialis (GM), gluteus medius (Gmed), soleus (Sol), tibialis anterior (TA) and vastus lateralis (VL). [7]*

3.3 Congruence between flexion-extension angles and muscle activations

The data that emerged from our analysis regarding the development of joint angles and corresponding muscle activations can be considered in agreement with each other and with what we expected.

At the instant of heel strike, the hip is in a condition of maximum flexion (indicated on the graph by the positive flexion-extension angle); it then passes into an extended configuration, indicated by a decrease in the flexion-extension angle, aided by the contraction of the vastus lateralis, the gluteus medialis for the first 20% of the cycle and the biceps femoris for the first 40%, to reach maximum extension (negative peak) just before the heel is released. In the flight phase, the hip returns to flexion, assisted by the contraction of the medial gluteus, vastus lateralis lateralis and biceps femoris in the last 20% of the cycle.

As far as the knee joint is concerned, it is first in extension, followed by slight flexion in the first 20% of the cycle. Maximum flexion occurs in the second half of the cycle, during the swing phase (60 - 80% of the cycle), corresponding to an activation of the tibialis anterior. After flexion, the knee passes into extension position, which remains until the next heel strike, supported by the contribution of activation of the vastus lateralis and medial gastrocnemius.

At the beginning of the gait cycle, the ankle is in a dorsiflexed configuration, subordinated to the contraction of the anterior tibialis, which favours forefoot support. Subsequently, the ankle performs a plantarflexion movement (first 5% of the cycle), when the anterior tibial is still active. In the thrust phase, it performs a dorsiflexion due to progressive and synergic contraction of the gastrocnemius and soleus. Between approximately 50 -60 % of the cycle, at the heel strike, there is a further plantaflexion and subsequent dorsiflexion, a position that is maintained until the end of the flight phase, as a result of the activation of the anterior tibialis.

3.4 Differences between medial gastrocnemius muscle activations observed by sampling the signal in proximal and distal position

The EMG signals acquired for the gastrocnemius muscle show some morphological discrepancies, which can be implied by the positioning of the sampling electrodes on the muscle itself.

In particular, from the image below [Fig. 9] it is possible to observe that, starting from 10% of the step cycle, the signal acquired with proximal electrodes presents an activation with a greater slope than that acquired with the distal electrode pair. In addition, the activation peak also varies in the two cases, both in terms of phase shift and in terms of activation: in the case of proximal acquisition, it is at a time instant just before 40% of the cycle, whereas for the distal signal it is immediately afterwards. It is hypothesised that this slight variation is due to a greater proximity of the proximal electrode to the innervation zone.

As far as the amplitude is concerned, it is not possible to consider these differences as significant, as the amplitude of the EMG signal depends on multiple factors apart from the level of activation, such as the possible presence of noise due to the sampling system. It can be assumed that the higher amplitude found on the distal electrode is attributable to the morphological conformation of the muscle itself. The gastrocnemius is a pinnate muscle, with fibres inclined with respect to the longitudinal course of the muscle, which insert on tendon endings at two different depth levels. It follows that the amplitude of the signal will be different at the two ends and the contribution due to the deeper half-fibre will be hidden (totally or partially) by the contribution from the superficial half-fibre [8]. Based on these considerations, it is possible to assume that the pair of electrodes placed distally (which detect the greater amplitude), are placed in correspondence with the more superficial fibres, while the pair of proximal electrodes are placed in correspondence with the deeper fibres.

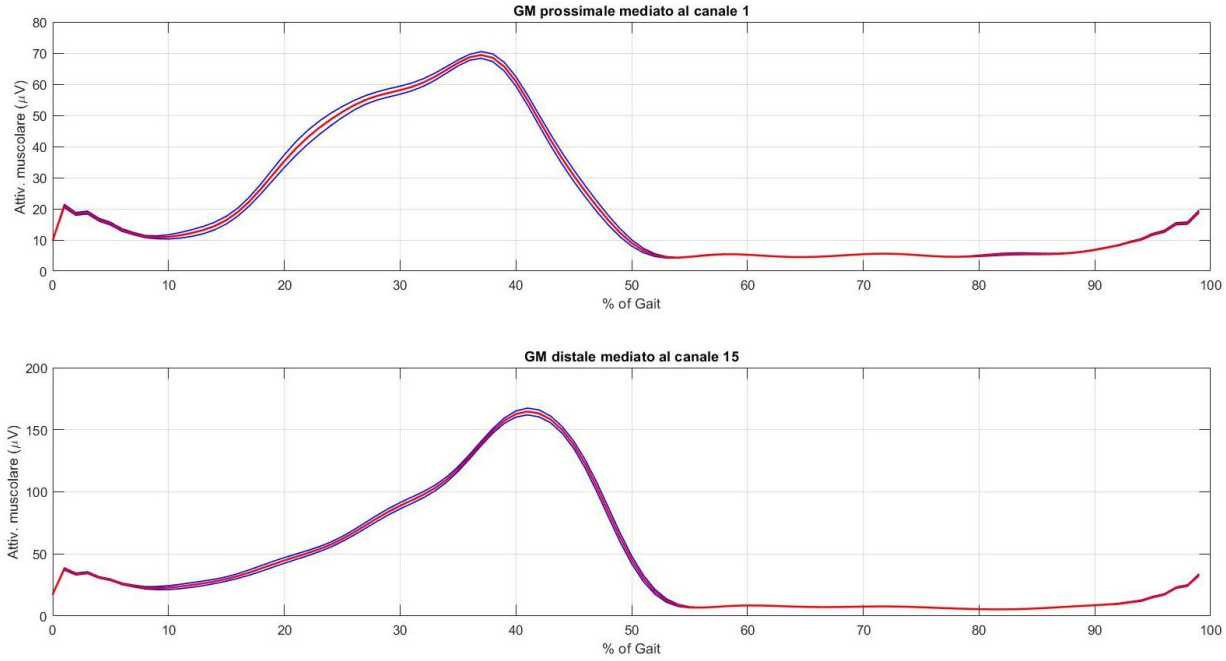

***Figure 9**: Average muscle activations, relative to acquisitions on the Medial Gastrocnemius muscle, with electrodes in proximal (Ch1) and distal (Ch15) position.*

4 Discussion and Conclusion

The aim of the analysis conducted is to evaluate the changes in joint angles, in particular flexion/extension and the corresponding muscle activations, as a function of the gait cycle. The occlusion of some markers from the field of view of the cameras caused the exclusion of several gait cycles from the dataset available for processing (approximately 46%). Nevertheless, the results obtained can be considered satisfactory and congruent with what has been found in the literature: having taken a healthy subject into analysis, in fact, we did not expect great differences in the trend of flexion-extension angles and their congruence with relative muscular activations.

Bibliography

[1] E. S. Grood and W. J. Suntay, 'A Joint Coordinate System for the Clinical Description of Three-Dimensional Motions: Application to the Knee', *Journal of Biomechanical Engineering*, vol. 105, no. 2, pp. 136 -144 · May 1983.

[2] Richard L. Pio, "Euler Angle Transformations", *IEEE TRANSACTIONS ON AUTOMATIC CONTROL*, vol. ac-11, no. 4, pp. 707-715 · October 1966.

[3] M. P. Kadaba, H. K. Ramakrishnan, M. E. Wotten 'Measurement of Lower Extremity Kinematics During Level Walking', *'Journal of Orthopaedic Research'*, vol. 8, no. 3, pp. 383 - 392 · 1990

[4] B. F. Mentiplay and R. A. Clark, 'Modified conventional gait model versus cluster tracking: Test - retest reliability, agreement and impact of inverse kinematics with joint constraints on kinematic and kinetic data', "Gait & Posture", pp 75 - 83 · 2018

[5] K. Y. Parikh et al,, Limb Employing Trans - Mechanism, '*International Journal of Recent Trends in Engineering & Research (IJRTER)'*, vol. 3, Issue 03 · 2017

[6] F. O. Barroso, D. Torricelli, J. C. Moreno et al, 'Shared muscle synergies in human walking and cycling', *Journal of Neurophysiology*, vol. 112, no. 8, pp. 1984 - 1998 · 2014

[7] Y. P. Ivanenko, R. E. Poppele and F. Lacquantini 'Five basic muscle activaction patterns account for muscle activity during human locomotion', *The Physiological Society*, pp.267 - 282 · 2004

[8] Taian M. M. Vieira, Ian D. Loram, S. Muceli, R. Merletti and D. Farina, Postural activation of the human medial gastrocnemius muscle: are the muscle units spatially localised?, 'Journal Physiology', vol. 589, pp. 431 - 443 · 2011